

Combined Quantum Chemical and MM-Approach to the *endo/exo* Selectivity of Diels-Alder Reactions in Polar Media ¹

Ingo Schlachter ^{a)}, Jochen Mattay ^{*a,b)}, Josef Suer ^{a)}, Udo Höweler ^{a)},
 Gudrun Würthwein ^{a)}, and Ernst-Ulrich Würthwein ^{a)}

a) Organisch-Chemisches Institut der Universität Münster, Corrensstr. 40, D-48149 Münster, Germany (fax: +49-251-83-9772)

b) Institut für Organische Chemie, Universität Kiel, Olshausenstr. 40, D-24098 Kiel, Germany (fax: +49-431-880-7410)

Abstract: The *endo/exo* selectivity of Diels-Alder reactions in water and methanol is studied with semiempirical methods using the SCRFF approach and a combined quantum chemical (transition state) and molecular mechanics (solvent molecules) method (QC/MM) to determine the effect of protic solvents on the transition state energies. Evidently, the number of hydrogen bonds that causes strong Coulomb interaction, discriminates heats of formation of transition states. The results indicate that the *s-cis/s-trans* conformation of acrylates controls the *endo/exo* selectivity.

Copyright © 1996 Elsevier Science Ltd

The effect of the solvent on the *endo/exo* selectivity ² of Diels-Alder reactions ³ was studied already in 1962 by Berson *et al.* in an extensive experimental exploration. ⁴ The *endo* adduct is preferentially obtained in reaction 1 (Fig. 1). In case of reaction 2, the major isomer can be selected by choosing a solvent of appropriate polarity. Buono and co-workers established a correlation between the conformation of an α,β -unsaturated carbonyl compound and its *endo/exo* selectivity. ⁵ Whenever such a cyclic compound is fixed in a *s-cis* arrangement, the reaction with cyclopentadiene (Cp) shows a high *exo* selectivity. ⁶ If a cyclic fixed *s-trans* system is examined, an excess of *endo* adducts is observed. This shows clearly that Alder's *endo* rule is not always obeyed.

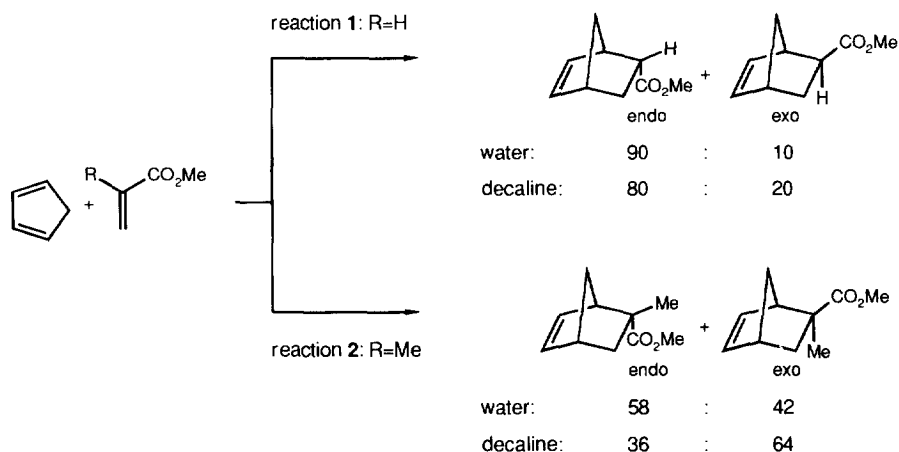


Figure 1. The diastereoselectivity of the sample reactions in dependence of solvent polarity

Calculation of Transition States in the Gas Phase

The determination of the transition state (TS) geometry by quantum chemical methods should give insight into the origin of the effect. Because of an overestimation of van der Waals repulsive forces at 2.2Å, the semi-empirical method MNDO gives unrealistic TS geometries with very unsymmetrical structures⁷. Whereas one of the forming bonds is almost completed (~1.6Å), the other distance is larger than the sum of the van der Waals radii of the respective centers (~3.4Å). MNDO's successor, AM1,⁸ is better suited for modeling this reaction with respect to the TS geometry including bond lengths.⁹ The findings are comparable to results of *ab initio* studies.¹⁰ On the other hand, AM1 reveals a strong preference for the formation of the *exo* product. All these calculations refer to the gas phase whereas the experimental product distribution depends strongly on the solvent⁴. Therefore, the dependence of the selectivity on the polarity of the solvent calls for a theoretical model that includes the effect of the solvent.

The Solvent Models

There are various models to account for electrostatic solute-solvent interactions in a "self consistent reaction field" (SCRF).¹¹ The partial charges of the solute placed in a cavity polarize the surrounding continuum characterized by its dielectric constant ϵ .¹² The induced electrostatic field of the continuum (reaction field) interacts with the molecular dipole moment of the solute. Thus an operator that accounts for the perturbation through the interactions with these dipole is added to the Hartree-Fock operator. We used this continuum model as implemented in GEOMOS¹³ to study the reactions **1** and **2** in water. By applying this approach to the reaction **1**, Ruiz-Lopez *et al.* found that there is a preference for the *exo* TSs.¹⁴

If solvent molecules are included explicitly, the number of internal degrees of freedom and thus the complexity of the problem is increased dramatically. In particular, the position and the orientation of the solvent molecules are defined less precisely due to the non-covalent nature of the solute-solvent interactions. In the supermolecule approach, only a limited number of solvent molecules is placed in the vicinity of those centers that are involved in the reaction and may be strongly polarized by the solvent. However, in the Diels-Alder reaction, these polarizable centers (ester group) are well separated from the reactive positions that take part in the bond breaking and forming processes (double bonds). It was found earlier that the use of AM1 in the supermolecule approach leads to unrealistic geometries and solvation energies.¹⁵

On adding more solvent molecules, the model system becomes too large to be studied by quantum chemical (QC) methods only. Therefore, a separation into a QC part (accounting for the solute, QC domain) and a molecular mechanics (MM) part (accounting for the solvent molecules, MM domain) provides a more versatile approach. Additionally, the multiminima problem arising due to an increasing number of solvent molecules that cannot be solved by optimizing a single geometry. A theoretical study by Blake and Jorgensen on the solvent effects of the Diels-Alder reaction between Cp and methyl vinyl ketone was carried out using Monte Carlo simulations. They placed the geometries along the minimum energy reaction path determined in the gas phase in solvents like water, methanol, and propane. By computing the changes in free energy of

solvation during the reaction, they showed that the transition barriers substantially decrease when going from vacuum to solution.¹⁶ However their model does not utilize a coupling between the solute and the solvent. Yet, it cannot accurately describe the change of the electronic structure of the solute due to the solvation.

Only an explicit coupling accounts for the electron re-distribution.¹⁷ We apply this approach to the sample reactions **1** and **2** studied by Berson *et al.*(Fig. 1).⁴

Computational Details

Method of Calculation

The total energy is determined by the contributions of the QC and the MM domain, and the interaction term (QC/MM) between both domains:

$$E(\text{tot}) = E(\text{QC}) + E(\text{QC} / \text{MM}) + E(\text{MM}) \quad (\text{Eq. 1})$$

The total interaction of the solute with the solvent is given by

$$E(\text{QC} / \text{MM}) = E_{\text{vdW}}(\text{QC} / \text{MM}) + E_{\text{hb}}(\text{QC} / \text{MM}) + E_{\text{coul}}^{\text{nuc}}(\text{QC} / \text{MM}) + E_{\text{coul}}^{\text{elec}}(\text{QC} / \text{MM}) \quad (\text{Eq. 2})$$

The van der Waals interactions between the atoms are derived from a Lennard-Jones potential

$$E_{\text{vdW}}(\text{QC} / \text{MM}) = \sum_{\mathbf{a}(\text{QC}), \mathbf{x}(\text{MM})} \epsilon_{\text{ax}} \left[\left(\frac{\sigma_{\text{ax}}}{r_{\text{ax}}} \right)^{12} - 2 \left(\frac{\sigma_{\text{ax}}}{r_{\text{ax}}} \right)^6 \right] \quad (\text{Eq. 3})$$

In this equation, r_{ax} gives the distance between the centers \mathbf{a} of the QC domain and \mathbf{x} of the MM domain. The two parameters are ϵ_{ax} , which corresponds to the depth of the minimum, and σ_{ax} , which is the separation at $E=0$. Whereas the repulsive forces are considered with r^{-12} , the attraction follows an r^{-6} potential.

The AMBER force field used in this study describes the interaction between acidic hydrogen atoms H in one domain and hydrogen bond acceptors in the other domain by the special hydrogen bonding term.

$$E_{\text{hb}}(\text{QC} / \text{MM}) = \sum_{\text{H}(\text{QC}/\text{MM}), \text{A}(\text{MM}/\text{QC})} \left(\frac{B_{\text{HA}}}{r_{\text{HA}}} \right)^{12} - \left(\frac{C_{\text{HA}}}{r_{\text{HA}}} \right)^{10} \quad (\text{Eq. 4})$$

In a comparison with eq. 3 it becomes evident that the attractive interactions decays faster with increasing distance due to the r^{-10} potential.

The third term of eq. 2 accounts for the Coulomb interaction between the nuclear charges $Z_{\mathbf{a}}$ (QC) and the partial charges $q_{\mathbf{x}}$ (MM)

$$E_{\text{coul}}^{\text{nuc}}(\text{QC} / \text{MM}) = \sum_{\mathbf{a}(\text{QC}), \mathbf{x}(\text{MM})} \left(\frac{Z_{\mathbf{a}} q_{\mathbf{x}}}{D r_{\text{ax}}} \right) \quad (\text{Eq. 5})$$

Finally, the non-additive Coulomb interaction between the electrons (QC) and the partial charges q_x (MM) effects directly the distribution of the electrons in the QC domain. It is incorporated into the one-electron Hamiltonian of the solute by

$$\hat{h}_i = \hat{h}_i^0 - \sum_{x(\text{MM})} \frac{q_x}{D r_{ix}} \quad (\text{Eq. 6})$$

This is the only term that cannot be calculated with previously parametrized data and is therefore non-additive. By enclosing this term, the complexity of the calculation is notably enlarged because a quantum chemical calculation is needed for each solute/solvent geometry. On the other hand, this term allows to determine the change of the electron distribution in the solute.

In Eq. 5 and 6, D denotes the dielectric function that can either correspond to the dielectric constant ϵ or can be chosen to be distance dependent via $D=\epsilon r$. In this work, we choose the latter with $\epsilon=1$.

The interaction of the solute with the solvent causes a perturbation of the isolated solute's wave function (Φ_{iso}), resulting in a wave function of higher energy (Φ_{per}) and in updated partial charges of the centers of the solute. The stabilization is effected only by MM interactions with the solvent. Fig. 2 only applies to the simple model used in this work.

Field *et al.* proposed a scheme (FBK) to couple semiempirical methods to a molecular mechanics environment.¹⁸ Their approach was modified by Vasiljev *et al.* (VBV)¹⁹. We have used a different combination of an AM1/MM approach (SH model)²⁰ which was tested in an *a priori* study of the tautomers and conformers of ascorbic acid in aqueous solution.¹⁷

In the semiempirical method AM1 the interaction between one s-orbital A (QC) and X (MM) can be exemplified by

$$(s_A s_A | s_X s_X) = \frac{-q_X}{\sqrt{R_{AX}^2 + \xi(\rho_A^0 + \rho_X^0)^2}} \quad (\text{Eq. 7})$$

with ρ as atom dependent parameter to screen the Coulomb potential at small distances. R_{AX} gives the distance between the nuclei. This formula assumes that the point charges at the MM centers can be

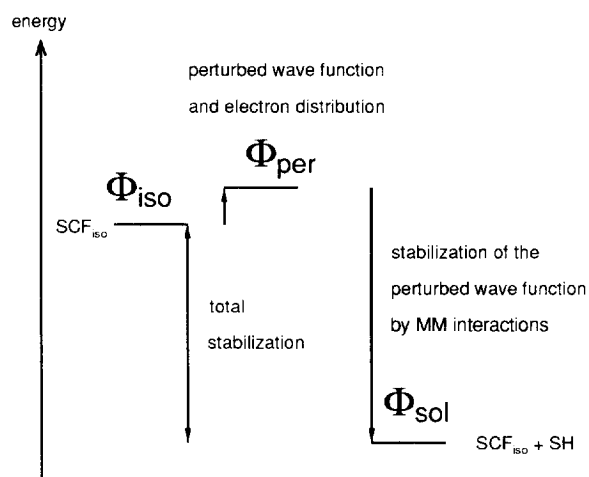


Figure 2. Influence of coupling with MM domain on wave function (SH model)

described as spherical shaped *s*-orbitals. In order to compare the different coupling models the factor ξ is introduced.¹⁹ For $\xi=1$ FBK proposed $\rho_x^0=0$ while VBV use ρ_x^0 for the centers in the MM domain but scaled the screening term by $\xi=0.1$. The SH model disregards this factor ($\xi=0$) and reduces to a single point charge approach. The FBK and VBV coupling models also consider off-diagonal elements

$$h_{\mu(A)\nu(B)} = -\delta_{AB} \sum_{X(MM)} \frac{\text{const.}}{\sqrt{R_{AX}^2 + \xi(\rho_A^0 + \rho_X^0)^2}} \quad (\text{Eq. 8})$$

so that all two center contributions within the NDDO approximation are accounted for. An analysis of the models shows that the total stabilization of the orbitals increase from FBK to SH, while the nuclear repulsion correspondingly decreases.

The determination of partial charges has been a matter of controversy for both the solvent²¹ and the solute.¹⁶ For a consistent description of the interactions across the QC/MM boundary as compared to the interior of the domains, we utilized a pattern that is based on the calculational methods used here. It applies not only for solvent molecules but also for the TS structures. Following a single point calculation with AM1, we scaled the point charges to fit the full quantum chemical dipole moment. Thus the resultant partial charge on oxygen (MM) in the water molecule is calculated to $-0.66 e$. The methyl group in methanol is reduced to a single atom (united atom). Its partial charge (MM) was assigned to $+0.2 e$, on oxygen (MM) $-0.5 e$.

The Procedure for the QC/MM Calculation

In the QC/MM calculations, we computed the relative stabilization energies for the transition states *exo s-trans* (XT), *exo s-cis* (XC), *endo s-trans* (NT), and *endo s-cis* (NC) as proposed earlier¹⁴ of the reactions **1** and **2** (Fig. 1) in liquid water and methanol. The procedure is summarized in Fig. 3. In order to solve the multim minima problem we applied molecular dynamics (MD) simulations to the solute/solvent system followed by subsequent optimizations of selected configurations.

MOPAC 6.0²² is used to determine the geometries of these isolated transition states. Using the key-word SADDLE, the previously optimized structures of Cp and the respective acrylate are brought into the vicinity of the transition state. The TS geometry is then located running the Eigenvector following routine (key-word TS) by applying the key-word PRECISE and requesting GNORM=0.1. Once a TS geometry is obtained for one configuration, the geometry is altered to the desired isomer and the TS procedure started again.²⁵ All resultant geometries are characterized by a normal coordinate analysis (key-word FORCE) as TSs by a single negative eigenvalue of the Hessian. The visualization showed that the corresponding vibration belongs to the movement from the starting compounds to the product (Table 1).²⁵

Throughout the following MD calculations for the solute/solvent systems, these geometries are kept fixed in space, while the solvent molecules are allowed to move according to the forces exerted by all atoms.

A single point calculation for the isolated TS and subsequent scaling provides the appropriate charge distribution. The calculations are performed with MAXIMOBY 3.3²³ running on an IBM-RS6000-32H workstation.

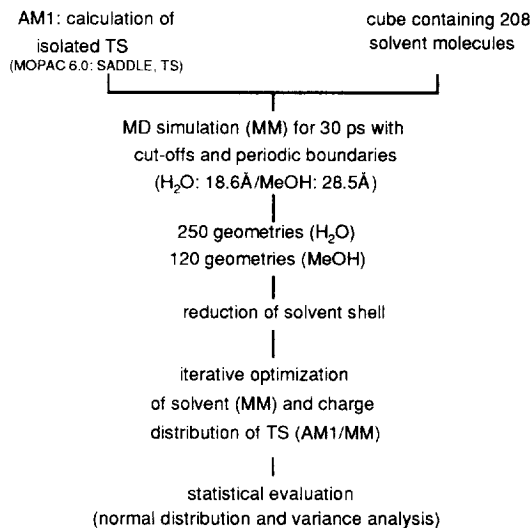


Figure 3. Procedure for the QC/MM calculation

In order to prepare starting geometries for the simulation, each TS structure is placed in a cubic box (18.6^3Å^3) containing 216 water molecules. This number is consistent with the density of water at room temperature and corresponds to a molecular volume of 3.1^3Å^3 . In case of methanol, the cube length equals 28.47Å containing 343 molecules (4.067^3Å^3). The eight molecules closest to the solute are removed to avoid high energy contributions at the start of the MD simulation.

AMBER potential functions²⁴ were used for the MM-MD calculations and the generalized center types of MOBY²⁵ were assigned to the QC atoms of the solute. After a conjugate gradient optimization of the solvent (5000 steps), temperature is raised by 10K per interval (100 steps) during the heating period from 0K until 300K are attained. Each time step takes 0.5fs that is used for heating period, equilibration time, and simulation. In these computations, periodic boundaries (with the minimum image approach) are applied as well as cut-offs of 9.3Å for the nonbonding interactions. The simulation is started after a short equilibration period of 300 time steps, which is sufficient because the simulation will only generate starting configurations for subsequent optimizations. It runs for 60000 time steps (30ps) at 300K; this temperature is adjusted every 100th cycle. During the time of the simulation, in case of water every 240th geometry, in case of methanol every 500th geometry is written to disk for later analysis, which results in 250 geometries for water, and 120 for methanol.

Those solvent molecules closest to the solute are subject to a further analysis of each geometry and the remaining molecules are removed. The energy of the transition states are calculated according to the QC/MM

coupling figure outlined above. The resultant systems are analyzed in an iterative optimization procedure for TS/solvent clusters with no periodic boundaries and cut-offs:

The first step consists of a single point calculation with AM1 for the TS geometry with coupling to the solvent to adjust the partial charges. Each time they are scaled to fit the full QC dipole moment. Subsequently, a full geometry optimization of the water molecules is performed. These cycles are terminated if the maximum change of a partial charge of a TS center drops below 5×10^{-4} electrons. The resulting heats of formation are used to evaluate the relative stability of the solvent.

In contrast to standard geometry optimizations for single molecules, the relative energy of the solute/solvent systems is determined as averages (mean values) of the heats of formation for the 250 (water) or 120 (methanol) configurations.

Statistical Analysis

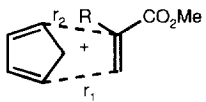
We performed the following tests to check whether the calculated differences of the energies are statistically significant²⁶. Initially, the Kolmogorov-Smirnov One-Sample test is used to compare the empirical cumulative distribution functions with the normal distribution function. Then, the equality of the variances of the four groups (XT, NT, XC, NC) is checked using Cochran's C-test. An analysis of variance combined with the multiple range tests (Scheffé method) is performed to detect significant differences among the four groups. The variances are not equal in case of reaction 1 with 100 water molecules. Therefore the Kruskal-Wallis test in combination with the multiple comparisons according to Nemenyi is used instead. The heat of formation of two groups are considered to be distinctable if their difference is greater than the limit calculated by the Scheffé method ($p=0.05$).

Results

Table 1 summarizes the data of the TSs as calculated by the AM1 method for the gas phase. Generally, the *exo* transition states are stabilized by ca. 1.5-2.0 kcal/mol. The geometries of the TSs for reaction 2 [$\Delta(r_1-r_2) \approx 0.3 \text{ \AA}$] are slightly more unsymmetrical than for reaction 1 [$\Delta(r_1-r_2) \approx 0.2 \text{ \AA}$]. The heats of formation and bond lengths are in accord with the results of Ruiz-Lopez *et al.*¹⁴

Table 2 and 3 summarize the results for reactions 1 and 2 in water and methanol using different methods of calculation. For easier comparison the conformation with the lowest ΔH_f is assigned $E_{rel}=0.00$ kcal/mol in each series. While the QC/MM procedure determines a mean value of ΔH for a TS, the SCRf approach computes a single free enthalpy ΔG . The experimentally observed value for T $\Delta\Delta S$ in case of reaction 1 in methanol is at room temperature 0.27 kcal/mol, for reaction 2 is T $\Delta\Delta S=0.31$ kcal/mol.⁴ Since statistically significant differences of heats of formation ($\Delta\Delta H \geq 1$ kcal/mol) exceed by far entropy contributions, the values for $\Delta\Delta S$ have been neglected.

Table 1: Characterization of Transition States in the Gas Phase



	Reaction 1				Reaction 2			
	XT	NT	XC	NC	XT	NT	XC	NC
ΔH_f [kcal/mol]	-4.62	-3.15	-5.27	-3.68	-8.08	-6.05	-8.33	-6.32
r_1 [Å]	2.02	2.02	2.02	2.02	1.98	1.99	1.98	1.98
r_2 [Å]	2.23	2.22	2.23	2.23	2.30	2.29	2.31	2.30
$\tilde{\nu}$ [cm ⁻¹] ^{a)}	i848	i853	i845	i850	i832	i843	i827	i837

^{a)} wave number for the lowest energy non-trivial vibration

Calculations for the Reactions in Water

Since the geometries of the isolated transition states are stationary points we optimized the surrounding solvent shells obtained from the MD simulation. In order to reduce the time needed for these optimization (250/H₂O, 120/MeOH) we had to limit the number of solvent molecules included. Therefore we report the results for reaction 1 in water for several sizes of the shells to determine the number of solvent molecules necessary to solvate the structures consistently. We introduce the following nomenclature. If an ensemble of 100 solvent molecules is considered in a single point QC/MM calculation, the label „cut 100“ is assigned, while „opt50“ is used for the iterative optimization of 50 solvent molecules.

Reaction 1 in water: For the isolated molecules, *exo* transition states (XC < XT) are calculated to be energetically favorable (Table 2). With the SCRf approach the XC structure is less stabilized by ca. 1.7 kcal/mol as compared to the other geometries. Thus, while an *exo* transition state is still lowest (XT) the ordering of XT and XC is reversed. Interestingly, the two *cis* conformations have nearly the same energy. According to the QC/MM procedures „cut 100“ and „opt 50“, no particular transition state is favoured. However, the *endo* transition states are increasingly stabilized with respect to the *exo* structures. So, the results for „opt 125“ show the same energies for XC and NC as they are found with the SCRf approach but the relative energies of XT and NT are exchanged, making NT the lowest energy transition state. Since this result can be obtained with less effort using the „opt 100“ procedure we take it as the reference for all systems.

The calculations also reveal some interesting features concerning the conformation of the dienophile in the transition state: Parallel to the stabilization of the *endo* TS when changing the medium from gaseous to liquid the *transoid* conformation is favoured. Whereas experimental studies of reaction 1 cannot provide any information about the favoured geometry Buono's correlation⁵ between the *endo/exo* selectivity and the *s-cis/s-trans* conformation of the dienophile support our computational results.

Table 2: Relative Energies of Transition States in Water

Experiment ²⁷	Reaction 1				Reaction 2				
	XT ^{a)}	NT	XC	NC	XT ^{a)}	NT	XC	NC	
	<i>endo</i> (0) / <i>exo</i> (1.27) ^{b)}				<i>endo</i> (0) / <i>exo</i> (0.12) ^{j)}				
Isolated	0.65	2.12	0	1.59	0.25	2.28	0	2.01	
SCRf ^{c)}	0	1.25	0.97	0.85	0.10	2.00	0	1.80	
QC/MM ^{d)} procedures	number ^{e)}								
Cut ^{f)}	100	0.50	0.02	0	1.19				
Opt ^{g)}	50	0	0.16	0.11	1.66				
Opt ^{g)}	100	1.17 ^{h)}	0 ^{h)}	0.68 ^{h)}	1.55 ^{h)}	0.19 ^{k)}	1.70 ^{k)}	0 ^{k)}	0.34 ^{k)}
Opt ^{g)}	125	1.60 ⁱ⁾	0 ⁱ⁾	1.03 ⁱ⁾	0.95 ⁱ⁾				

a) XT=*exo s-trans* conformation of acrylate, NC=*endo s-cis*; b) $\Delta\Delta G$ for selectivity 9.3:1; c) calculations with GEOMOS; d) average energies for 250 geometries; e) number of water molecules considered; f) single point calculation at geometries from MD resultant ΔH_f ca. -30 kcal/mol; g) iteratively optimized geometries resultant ΔH_f ca. -46 - -51 kcal/mol; h) statistically significant difference at 0.97 kcal/mol; i) statistically significant difference at 1.10 kcal/mol; j) selectivity 1.4:1; k) statistically significant difference at 1.22 kcal/mol

Reaction 2 in water: The gas phase calculations also determine the *exo* transition states to be lower in energy by ca. 2.0 kcal/mol and only a small difference between *cis* and *trans* structures. In the SCRf model the transition states are stabilized uniformly leading to the same result (XT≈XC<NC≈NT). In the QC/MM method NC is strongly stabilized getting close in energy to the *exo* transition states whose relative energies are not changed. Whereas in the QC/MM approach NC is significantly more stabilized than NT, neither for the isolated transition states nor with the SCRf method a preference for any conformation is determined.

Calculations for the Reactions in Methanol

In Table 3 we report the results for the calculations in methanol. The heats of formation calculated by the SCRf approach are almost identical with the results in water.

Table 3: Relative Energies for the Transition States in Methanol

Experiment ²⁷	Reaction 1				Reaction 2			
	XT ^{a)}	NT	XC	NC	XT ^{a)}	NT	XC	NC
	<i>endo</i> (0) / <i>exo</i> (1.4) ^{b)}				<i>endo</i> (0.1) / <i>exo</i> (0) ⁱ⁾			
Isolated	0.65	2.12	0	1.59	0.25	2.28	0	2.01
SCRf ^{c)}	0	1.26	0.88	0.86	0.09	2.02	0	1.81
QC/MM ^{d)}	4.31 ^{e)}	0 ^{e)}	4.41 ^{e)}	1.89 ^{e)}	0 ^{g)}	2.40 ^{g)}	3.05 ^{g)}	0.25 ^{g)}

a) XT=*exo s-trans* conformation of acrylate, NC=*endo s-cis*; b) $\Delta\Delta G$ for selectivity 7:1; c) calculations with GEOMOS; d) average energies for 120 geometries optimized with 100 methanol molecules; e) statistically significant difference at 1.32 kcal/mol; f) $\Delta\Delta G$ for selectivity 0.7:1; g) statistically significant difference at 1.24 kcal/mol

In case of reaction **1** the QC/MM procedure determines **NT** to be the most stable TS followed by **NC**. For reaction **2** **XT** and **NC** nearly have the same energy. The splitting of the energies is surprisingly large as compared to the results for water as solvent.

Discussion

Compared to the gas phase the SCRF model favours the *exo* TSs in all considered reactions though the energy gap between the *endo* and the *exo* TSs is decreased. Additionally, this method shows only little sensitivity to solvent polarity because almost identical values are obtained for each transition state. Concluding from these data the SCRF approach seems to be limited to processes of which specific interactions with solvents can be disregarded. The results reported by Sustmann and Sicking for Diels-Alder reactions of 2-azabutadiene using GEOMOS²⁸ may be taken not only as one successful application of the SCRF approach but also as a support of its limitation. Due to the discrepancy between the SCRF results and the experimental data for reaction **1** in water Ruiz-Lopez *et al.* concluded that specific interactions like hydrogen bonding are crucial for Diels-Alder reactions in polar protic solvents.²⁹

For reaction **1** in water, **NT** is found to be the most stable transition state according to the QC/MM models supporting the experimentally observed *endo* selectivity. In addition, the difference of 1.2 kcal/mol to **XT** is statistically significant. Thus, the ordering of **NT** and **XT** is reversed with respect to the SCRF results. Ruiz-Lopez reported the transoid transition state to be energetically favoured by using ab initio/SCRF procedures.²⁹ However, our calculations give a deviation of **NT** to **XC** which amounts ca. 0.7 kcal/mol. Therefore we assume that the *s-cis* and *s-trans* conformers must be considered separately for the evaluation of the *endo/exo* selectivity. In case of reaction **2** our results are consistent with the experimentally observed unselectivity because three (**XC**, **XT**, **NC**) of four transition states are determined to have only minor differences.

Again it is **NT** which is calculated to be energetically favoured in case of reaction **1** in methanol. Since the experimentally observed energy gap (referring to $\Delta\Delta G$) is only 1.4 kcal/mol, the results clearly overemphasize the *endo* selectivity because both *endo* transition states are significantly more stable than the corresponding *exo* transition states ($\Delta\Delta H \geq 2.5$ kcal/mol). For reaction **2** no selectivity is found because **XT** and **NC** have similar energies. The generally larger energy differences for the reactions in methanol and a lower quality of the results have to be attributed to the smaller set of geometries (120) as compared to the calculations in water (250) and the united atom approximation for the solvent (no explicit hydrogens at the carbon).

We now turn to the factors which stabilize the transition states such as dipole moment, charge distribution and hydrogen bonds. Focusing on reaction **1** in water, purely electrostatic interactions should give rise to a correlation between the relative heat of formation and the dipole moment of a transition state (Table 4). Indeed, the energetically most stable transition states (**NT**) has the highest dipole moment (QC/MM: 4.54 Debye) but there is only a minor difference to the value of **XT** (4.40 Debye). In reaction **2**, both, the change (compared to

the isolated transition states) and the absolute dipole moments calculated for **NT** and **NC** are almost identical and cannot provide a rationalization for the splitting of the corresponding heats of formation as well.

Table 4: Dipole Moments [Debye] of Transition States Calculated by Various Methods with AM1 for the Reactions **1** and **2** in Water and in the Gas Phase.

	Reaction 1				Reaction 2			
	XT	NT	XC	NC	XT	NT	XC	NC
Isolated ^{a)}	2.84	2.95	1.87	2.71	2.71	2.79	1.95	2.55
SCRf	3.24	3.33	- ^{c)}	2.96	3.12	3.19	2.20	2.88
QC/MM ^{b)}	4.40	4.54	3.04	3.96	4.76	4.56	3.80	4.54

a) dipole moments based on point charges calculated by AM1; b) based on all 250 optimized geometries (with 100 water molecules); c) GEOMOS calculates an unreal value of 1100

Analyzing the partial charges shows that the ester group is the strongest polarized part of the molecule.¹ The highest change of the partial charges of the carbonyl oxygen is observed for **NT** in case of reaction **1** in water (Table 5). In methanol both the absolute values as well as the differences are smaller than in water. Obviously, the QC/MM model accounts for the lower polarity of methanol as compared to water. The corresponding change at the sp³ oxygen will not be discussed because it does not exceed 0.02 electrons.

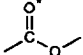
Table 5: Relative Change of Partial Charges of the Carbonyl Oxygen according for the Reactions **1** and **2** in Water and Methanol (QC/MM^{a)}) Compared to Values in the Gas Phase (AM1).

	Reaction 1				Reaction 2			
	XT	NT	XC	NC	XT	NT	XC	NC
Water	-0.13	-0.14	-0.11	-0.12	-0.15	-0.14	-0.15	-0.16
Methanol	-0.07	-0.11	-0.05	-0.08	-0.09	-0.08	-0.06	-0.10

a) based on all 250/120 optimized geometries (with 100 solvent molecules)

Table 6 gives the total number of water hydrogens within a distance range to form hydrogen bonds to the carbonyl oxygen. These numbers correspond to those reported by Blake and Jorgensen who calculated an average of 2 - 2.5 hydrogen bonds for methyl vinyl ketone¹⁶. **NT** shows the highest average per atom and allows for the highest density of hydrogens in the 1.6 to 1.8 Å interval with strongest Coulomb interactions. This explains the more pronounced accumulation of charge on the carbonyl oxygen (Table 5) and the larger stabilization of the **NT** structure (Table 2) and thus the energetic ordering of the solvated transition states.

Table 6: Total Number of Hydrogen Atoms^{a)} near the Carbonyl Oxygen for Reactions 1 and 2 in Water

 Distance Intervals [Å]	Reaction 1				Reaction 2			
	XT	NT	XC	NC	XT	NT	XC	NC
1.6 - 1.8	161	195	147	114	346	348	341	391
1.8 - 2.0	393	410	347	401	260	222	243	196
2.0 - 2.2	57	48	45	81	24	27	17	13
Sum 1.6 - 2.2	611	653	539	596	630	597	601	600
Average per atom	2.44	2.61	2.16	2.38	2.52	2.39	2.40	2.40

a) based on all 250 optimized geometries (with 100 water molecules)

For reaction 2 even more close hydrogen bonding contacts (interval 1.6 to 1.8 Å) are found resulting in the larger polarization of the carbonyl group (Table 5) and the higher dipole moments (Table 4) when compared to the transition states of reaction 1. The larger stabilization of NC compared to the other three structures can be rationalized by its very high number of close contacts. The average number of hydrogen bonds are very similar for all four transition states ($\Delta < 0.15$) indicating no preference for any conformation. Surprisingly, these numbers are comparable to those of reaction 1, which would not have been expected for steric reasons.

Thus, the number of hydrogen bonds give a good rationalization for the changes in the energetic ordering of the transition states. Table 5 and 7 clearly show that this also applies to the reactions in methanol. In reaction 1 the significantly higher number of hydrogen bonds in the *endo* transition states correlates with the stronger polarization of their carbonyl groups and their larger stabilization by the solvent. This holds for reaction 2 also where the most stabilized structures (XT, NC) allow for the largest number of hydrogen bonds. It should be noted that the number of hydrogen bonds is significantly lower in methanol as compared to water, which was also observed by Jorgensen *et al.* in the case of methyl vinyl ketone³⁰.

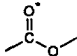
Finally, some features concerning the conformation of the dienophile will be discussed. Spectroscopic studies show that the *s-cis* conformation of acrylates is more stable in the gas phase³¹ which is supported by *ab initio* calculations³², whereas Buono's⁵ correlation reveal the opposite for solution. It is also known that methyl acrylates prefer the *s-trans* conformation in solution³³. Little is known about the conformations of methyl methacrylates (reaction 2). However the additional methyl group is expected to shield the carbonyl group from forming efficient hydrogen bonds in either conformation. Thus, it can be assumed, that no particular conformation will dominate in solution.

Thus, the NT conformation can easily be adopted in reaction 1 which is energetically more favorable than XT (1.2 kcal/mol). This results in a pronounced *endo/exo* selectivity. Any conformation can be equally well reached in reaction 2 leading to the energetically similar transition states found in our calculation, consequently no selectivity is predicted.

This supports the correlation between dienophile conformation and product configuration stated by Buono⁵ and gives a new reasoning for the origin of the *endo/exo* selectivity and replace the argument of secondary orbital overlap which was already doubted by Sustmann in 1992.³⁴

Table 7: Total Number of Hydrogen Atoms ^{a,b)} around the Carbonyl Oxygen for the Reactions 1 and 2 in

Methanol



Distance Intervals [Å]	Reaction 1				Reaction 2			
	XT	NT	XC	NC	XT	NT	XC	NC
1.6 - 1.8	13	27	16	16	19	17	6	14
1.8 - 2.0	98	198	73	145	160	143	107	190
2.0 - 2.2	1	2	0	3	2	3	2	3
Sum 1.6 - 2.0	112	227	89	164	181	163	115	207
Average per atom	0.93	1.89	0.74	1.37	1.51	1.36	0.96	1.73

a) based on all 120 optimized geometries (with 100 methanol molecules)

Conclusion

In summary, the differences computed by the QC/MM procedure are close to experimentally determined selectivities in three of four reactions. With regard to our results and analysis, we conclude that the conformation of the acrylates and the transition state determine the *endo/exo* selectivity. An analysis of the origin of the effect showed that polar solvents increase the dipole moment of transition states of 50-70% compared to the gas phase. The effect of increased partial charges becomes most evident at the ester group. This functional group also interacts through hydrogen bonds with protic solvents which is in synergistic relation with strong Coulomb interactions. By different stabilization, both contributions induce an energetic differentiation of the TSs resulting in the experimentally observed *endo/exo* selectivity.

The approach presented here applies QC and MM methods simultaneously for the full TS-solvent system rather than using properties determined for the isolated reactants. Our method includes the relaxation of the solvent molecules, which is necessary to treat the interactions between the fixed transition state structures and the solvent adequately.

Acknowledgements

We gratefully acknowledge financial support by the Deutsche Forschungsgemeinschaft and the Fonds der Chemischen Industrie.

References:

1. Partly presented at the 1st European Conference on Computational Chemistry, Nancy, France, 23.-27.05.1994; AIP Conference Proceedings 330, E.C.C.C.1, Computational Chemistry, F. Bernardi, J.L. Rivail (Eds.), Amer. Inst. of Physics, Woodbury, NY, 1995, p. 145-150. Schlachter, I., part of the Ph.D. thesis, Universität Münster, 1995.

2. Gaede, B.; Balthazor, T.M. *J. Org. Chem.* **1983**, 48, 276-277 and references cited therein.
3. Sauer, J.; Sustmann, R. *Angew. Chem.* **1980**, 92, 773-801; *Angew. Chem. Int. Ed. Engl.* **1980**, 19, 779-807.
4. Berson, J.A.; Hamlet, Z.; Mueller, W.A. *J. Am. Chem. Soc.* **1962**, 84, 297-304.
5. Fotiadu, F.; Michel, F.; Buono, G. *Tetrahedron Lett.* **1990**, 31, 4863-4866.
6. a) Mertes, J.; Mattay, J. *Helv. Chim. Acta* **1988**, 71, 742-748,
b) Mertes, J.; Mattay, J.; Maas, G. *Chem. Ber.* **1989**, 122, 327-330,
c) Kneer, G.; Mattay, J. *Synlett* **1990**, 145-147,
d) Kneer, J.; Mattay, J.; Raabe, G.; Krüger, C.; Lauterwein, J. *Synthesis* **1990**, 599-603,
e) Roush, W.R.; Brown, B.B. *J. Org. Chem.* **1992**, 57, 3380-3387,
f) Pyne, S.G.; Dikic, B.; Gordon, P.A.; Skelton, B.W.; White, A.H. *Austr. J. Chem.* **1993**, 46, 73-93.
7. Branchadell, V.; Orti, J.; Ortuño, R.M.; Oliva, A.; Bertran, J.; Font, J.; Dannenberg, J.J. *J. Org. Chem.* **1991**, 56, 2190-2193.
8. Dewar, M.J.S.; Zoebisch, E.G.; Healy, E.F.; Stewart, J.J.P. *J. Am. Chem. Soc.* **1985**, 107, 3902-3909.
9. Oliva, A.; Bertran, J.; Sodupe, M.; Dannenberg, J.J. *J. Org. Chem.* **1989**, 54, 2488-2490.
10. Jorgensen, W.L.; Lim, D.; Blake, J.F. *J. Am. Chem. Soc.* **1993**, 115, 2936-2942.
11. Wong, M.W.; Frisch, M.J.; Wiberg, K.B.; *J. Am. Chem. Soc.* **1991**, 113, 4776-4782.
12. Karelson, M.M.; Katritzky, A.R.; Szafran, M.; Zerner, M.C. *J. Org. Chem.* **1989**, 54, 6030-6034 and references cited therein.
13. Rinaldi, D.; Hoggan, P.E.; Cartier, A. *QCPE* 584.
14. Cativiela, C.; Garcia, J.I.; Mayoral, J.A.; Royo, A.J.; L. Salvatella, Assfeld, X.; Ruiz-Lopez, M.F. *J. Phys. Org. Chem.* **1992**, 5, 230-238.
15. Coitiño, E.L.; Irving, K.; Rama, J.; Iglesias, A.; Paulino, M.; Ventura, O.N. *J. Mol. Struct. (THEOCHEM)* **1990**, 210, 405-426.
16. Blake, J.F.; Jorgensen, W.L. *J. Am. Chem. Soc.* **1991**, 113, 7430-7432 and references cited therein.
17. Höweler, U.; Bäcker, Th.; Klessinger, M.; Eckert-Maksic, M.; Maksic, Z.B. *Croat. Chem. Acta* **1990**, 64, 539-549.
18. Field, M.J.; Bash, P.A.; Karplus, M. *J. Comp. Chem.* **1990**, 11, 700-733.
19. Vasilyev, V.V.; Blizlyuk, A.A.; Voityuk, A.A. *Int. J. Quantum Chem.* **1992**, 44, 897.
20. Suer, J.; Höweler, U. *unpublished results*.
21. Jorgensen, W.L. *J. Am. Chem. Soc.* **1981**, 103, 335-340 and references cited therein.
22. MOPAC 6.0, *QCPE* 455, **1990**.
23. Program MAXIMOBY 3.3: Batch-orientated version of MOBY, Höweler, U.; CHEOPS, Münster **1995**.
24. Weiner, S.J.; Kollman, P.A.; Case, D.A.; Nguyen, D.T. *J. Comp. Chem.* **1986**, 7, 230.
25. MOBY 1.6, Höweler, U.; Springer Verlag **1995**.
26. Sachs, L. *Angewandte Statistik*, 6. Auflage, Springer-Verlag, Berlin **1984**.
27. Breslow, R.; Maitra, U.; Rideout, D. *Tetrahedron Lett.* **1983**, 24, 1901-1904.
28. Sustmann, R.; Sicking, W.; Lamy-Schelkens, H.; Ghosez, L. *Tetrahedron Lett.* **1991**, 32, 1401-1404.
29. Ruiz-Lopez, L.; Assfeld, X.; M.F.; Garcia, J.I.; Mayoral, J.A.; Salvatella *J. Am. Chem. Soc.* **1993**, 115, 8780-8787.
30. Jorgensen, W.L.; Lim, D.; Blake, J.F. *J. Org. Chem.* **1994**, 59, 803-805
31. Carmona, P.; Moreno, J. *J. Am. Chem. Soc.* **1982**, 104, 177-179.
32. Loncharich, R.J. *J. Am. Chem. Soc.* **1987**, 109, 14-23.
33. George, W.O.; Hassid, D.V.; Maddams, W.F. *J. Chem. Soc., Perkin Trans 2* **1972**, 400-404.
34. Sustmann, R.; Sicking, W. *Tetrahedron* **1992**, 48, 10293-10300.

(Received in Germany 31 May 1996; revised 11 October 1996; accepted 16 October 1996)